

# Effect of Particle Size on Drug Loading and Release Kinetics of Gefitinib-Loaded PLGA Microspheres

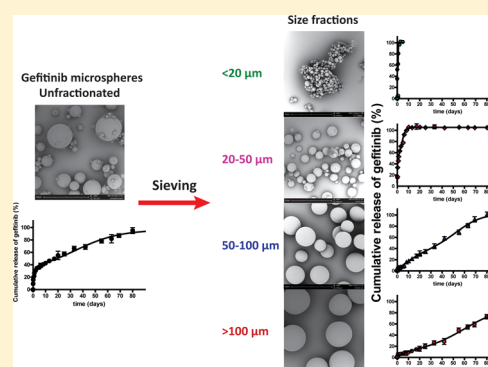
Weiluan Chen, Amelia Palazzo, Wim E. Hennink, and Robbert J. Kok\*

Department of Pharmaceutics, Utrecht Institute for Pharmaceutical Sciences, Utrecht University, 3584 CG Utrecht, The Netherlands

## Supporting Information

**ABSTRACT:** Polymeric microspheres have gained widespread application as drug eluting depots. Typically, drug-loaded polymeric microspheres are prepared by oil-in-water emulsification which yields a product with a broad size distribution. The aim of the present study was to investigate the properties of different size-fractions of drug-loaded microspheres, in order to delineate whether particle size governs drug loading efficiency and release profile. Gefitinib-loaded PLGA-based microspheres were prepared using an oil-in-water solvent evaporation method and wet-sieved to obtain well-defined size fractions of  $5 \pm 1$ ,  $32 \pm 4$ ,  $70 \pm 3$ , and  $130 \pm 7$   $\mu\text{m}$ , respectively. The average drug loading of unfractionated microspheres was  $6.3 \pm 0.4\%$  w/w, while drug loading of sieved fractions ranged from  $2.4 \pm 0.3$  to  $7.6 \pm 0.9\%$  w/w for smallest to largest microparticles. X-ray diffraction (XRD) and differential scanning calorimetry (DSC) analysis demonstrated that gefitinib was amorphously dispersed in the PLGA matrix, with no apparent shift in the  $T_g$  of PLGA indicating the absence of direct molecular interactions of the drug and polymer due to the formation of small drug particles embedded in PLGA. *In vitro* drug release was studied with microspheres embedded in dextran hydrogels to avoid their aggregation during the incubation conditions. Microspheres smaller than  $50$   $\mu\text{m}$  showed rapid diffusion-based release reaching completion within 2 days when particles have not degraded yet. Larger microspheres, however, showed a sigmoidal release pattern that continued for three months in which diffusion (early stage) as well as particle erosion (later stage) governed drug release. Scanning electron microscopy (SEM) and polymer degradation data showed that larger microspheres degraded faster than smaller ones, which is in line with autocatalytic PLGA degradation upon acidification within the core of microparticles. In conclusion, we showed that different size-fractions of drug-loaded microspheres showed quite distinct drug loading and release kinetics. Control of microparticle size by fractionation is therefore an important determinant for obtaining well-defined and reproducible sustained release depots.

**KEYWORDS:** polymeric microspheres, release kinetics, gefitinib, diffusion, erosion, biodegradable, drug depots



## 1. INTRODUCTION

Biodegradable polymeric microspheres have been extensively investigated as delivery systems for a variety of molecules such as peptides and pharmaceutical proteins<sup>1–3</sup> and hydrophobic drugs.<sup>4–6</sup> Tailoring the chemical and physical properties of polymers allows control over the release properties of such drug eluting systems, which can be modulated over the required time period, for instance, from days to several weeks to over a year.<sup>2</sup> Poly(lactide-co-glycolide) (PLGA) has been one of the most frequently used biodegradable polymers for the development of drug-loaded microspheres systems.<sup>5,7</sup> PLGA microspheres are usually produced by an emulsification process in which the drug and polymer are emulsified into micro-sized droplets that solidify upon extraction of the organic solvent from the dispersed phase. Classical production by high-speed emulsifiers or sonication typically produces particles with a wide range in particle size and internal and external morphology,<sup>8,9</sup> depending on the formulation and process parameters. More recent production processes involve membrane sieving and microfluidic devices resulting in so-called monodisperse microspheres

with a narrow size distribution, referred to as monospheres.<sup>10–12</sup> Drug release from biodegradable polymeric microspheres largely depends on diffusion, particle erosion, or a combination of these processes.<sup>13–16</sup>

A significant amount of work has been done on the mathematical modeling of drug release profiles from polymeric microspheres, to predict drug release rates and provide insight into the fundamental processes that govern release.<sup>15,17–19</sup> However, the physical and chemical processes involved in drug release from biodegradable polymeric matrixes are complex, and factors such as drug solubility and its diffusion coefficient in the polymer matrix may change in time in response to polymer chain scission and influx of water. Although mechanistic models for drug-eluting depots such as the Higuchi model or the Korsmeyer–Peppas model have been used to describe drug

**Received:** October 5, 2016

**Revised:** November 29, 2016

**Accepted:** December 14, 2016

**Published:** December 14, 2016

release profiles from microspheres,<sup>20–22</sup> most release profiles are best described by nonmechanistic sigmoidal curve fitting models.<sup>23</sup> We now hypothesize that different properties of larger and smaller microspheres contribute to the complex drug release profile of polydisperse microspheres, while such considerations do not apply, or only to a lesser extent, to macroscopic sustained release formulations. Such differences may relate to the final surface/volume ratio of the polymeric microspheres but may also originate from differences in the rates of solvent extraction between smaller and larger emulsion droplets during preparation affecting the drug loading of these particles. The objective of the present study is to investigate the relationship between particle size and drug loading and release profiles of well-defined size fractions obtained from polydisperse microspheres. Our method of microsphere preparation is commonly applied for the majority of drug-loaded microparticles and are therefore relevant for obtaining better reproducible results with amphiphilic drug compounds.

In this study, we used gefitinib as an amphiphilic model drug (Figure 1), which is a low molecular weight inhibitor of the

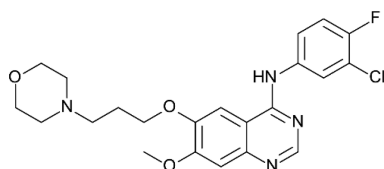


Figure 1. Chemical structure of gefitinib.

intracellular tyrosine kinase domain of epidermal growth factor receptor (EGFR) that has been approved for the treatment of EGFR-positive metastatic nonsmall cell lung cancer (NSCLC).<sup>24</sup> Gefitinib-loaded polymeric microspheres can be of potential benefit for the local treatment of NSCLC when implanted in a stent-like device. We prepared gefitinib-loaded microspheres by a single w/o emulsion method similar to a previously described method for the kinase inhibitor imatinib<sup>25</sup> and fractionated the obtained polydisperse product into well-defined size fractions by membrane sieving. The resulting subsets of polymeric microspheres were studied for their drug-loading, physicochemical properties, and drug release profiles.

## 2. EXPERIMENTAL SECTION

**2.1. Materials.** PLGA 5004A (acid terminated, lactide/glycolide molar ratio 50:50, IV = 0.4 dL/g) was obtained from Corbion Purac Biomaterials, The Netherlands. Gefitinib (free base, >99%) was purchased from LC laboratories, USA. Poly(vinyl alcohol) (PVA;  $M_w$  = 30–70 000 g/mol, 87–90% hydrolyzed), disodium hydrogen phosphate ( $\text{Na}_2\text{HPO}_4$ ) and sodium azide ( $\text{NaN}_3$ , BioUltra,  $\geq 99.5\%$ ) were purchased from Sigma-Aldrich (Germany). Phosphate buffered saline (PBS pH 7.4, 0.049 M  $\text{NaH}_2\text{PO}_4$ , 0.099 M  $\text{Na}_2\text{HPO}_4$ , 0.006 M NaCl) was purchased from Braun (Melsungen AG, Germany), dichloromethane (DCM), tetrahydrofuran (THF) and acetonitrile were purchased from Biosolve (Valkenwaard, The Netherlands). Dextran (from *Leuconostoc mesenteroides*, T40,  $M_w$  = 40,000), glycidyl methacrylate (GMA), ammonium peroxydisulfate (APS), and  $N,N,N',N'$ -tetramethylethylenediamine (TEMED) were obtained from Fluka Chemie AG, Buchs, Switzerland. 4-( $N,N$ -Dimethylamino) pyridine (DMAP, 99%) was from Acros Chimica, Geel, Belgium. Dialysis tubes

(cellulose,  $M_w$  cutoff 12,000–14,000) were purchased from Medicell International Ltd., London, England.

**2.2. Preparation of Gefitinib-Loaded PLGA Microspheres.** Gefitinib-loaded PLGA microspheres were prepared by a single o/w emulsification as described previously.<sup>25,26</sup> PLGA 5004A (5 g) was dissolved in 10 mL of dichloromethane (DCM). Since gefitinib has a low solubility in DCM (15 mg/mL), DMSO was used as cosolvent. Gefitinib was dissolved in dimethyl sulfoxide (DMSO) and heated at 60 °C for 10 min to obtain stock solution of 200 mg/mL. After cooling, 2.5 mL of this gefitinib stock solution (corresponding with 500 mg of gefitinib) was mixed with the PLGA solution (final gefitinib/PLGA ratio was 1:10 w/w). The resulting organic phase was transferred into a plastic syringe and dropwise emulsified (6 min) into 100 mL of 2% PVA aqueous solution while stirring at a rate of 30,000 rpm using an IKA homogenizer (IKA Labortechnik Sraufen, Germany). Next, the suspension was stirred overnight at room temperature using a magnetic stirrer (500 rpm) to extract and evaporate DCM. Microspheres were collected by centrifugation (4000g for 3 min, Laboratory centrifuge, 4K15 Germany), washed three times with 50 mL of distilled water, and lyophilized overnight. Blank microspheres without gefitinib were prepared in a similar manner.

Lyophilized microspheres were fractionated by wet-sieving using standardized square mesh sieves of 100, 50, and 20  $\mu\text{m}$  mesh sizes (Nickel precision filters, Stork Veco BV, Eerbeek, The Netherlands), lyophilized again, and stored at  $-20$  °C until further use.

**2.3. Characterization of the Microspheres.** **2.3.1. Determination of Microspheres Sizes.** Particle size distributions of three independently prepared batches of gefitinib microspheres and their corresponding size-fractions were determined by an AccuSizer 780 (Optical particle size, Santa Barbara, California, USA). Particle sizes are reported as volume weighted mean diameters (vol-wt mean), while polydispersity is expressed as span value (SP) calculated with the following formula:  $\text{SP} = (d_{90} - d_{10})/d_{50}$ , where  $d_{90}$  is the particle diameter at 90% cumulative size,  $d_{10}$  is the particle diameter at 10% cumulative size, and  $d_{50}$  is the particle diameter at 50% cumulative size.<sup>27</sup> A high span value indicates a wide distribution in size (polydispersity), while a lower span value indicates a narrow size distribution (monodispersity). The size distribution is considered as narrow for span values <0.45.<sup>28</sup> Aliquots of approximately 10 mg of microspheres suspended in 1 mL of water were assayed. A minimum of 9000 microspheres were analyzed for each sample.

**2.3.2. Determination of Gefitinib Content in the Microspheres.** The gefitinib loading of unfractionated and fractionated microspheres was determined by dissolving accurately weighed amounts of microspheres of approximately 3 mg in 10 mL of DMSO. Gefitinib concentrations in these samples were measured by high performance liquid chromatography (HPLC) using a C18 column (4.6  $\times$  150 mm, 5  $\mu\text{m}$  particle size; Sunfire, Ireland) and a mobile phase of acetonitrile/methanol/water in ratio of 20:23:57 v/v/v, complemented with TFA (0.3% w/v), at a flow rate of 1.0 mL/min. Gefitinib standards (1–150  $\mu\text{g}$ /mL dissolved in DMSO) were used for calibration, and detection was done at 254 nm. Loading capacity (LC) and encapsulation efficiency (EE) were calculated using the following equations:

$$\text{LC (\%w/w)} = \frac{\text{mass of drug microspheres}}{\text{total mass of microspheres}} \times 100$$

$$\text{EE (\%)} = \frac{\text{loading content (LC\%/w/w)}}{\text{initial drug loading (\%/w/w)}} \times 100$$

**2.3.3. Scanning Electron Microscopy (SEM).** Samples were glued on 12 mm diameter aluminum sample holders using conductive carbon paint (Agar scientific Ltd., England) and covered by a platinum layer (4 nm) under vacuum using an ion coater. The morphology of the microspheres was examined by scanning electron microscopy (SEM, Phenom, FEI Company, The Netherlands).

**2.3.4. Thermal Gravimetric Analysis (TGA).** Residual solvent content of the microspheres was determined by thermal gravimetric analysis (TGA) using a Q Series instrument (Q50, TA Instruments, USA). Accurately weighed amounts of around 15 mg of freeze-dried microspheres were loaded into aluminum pans and heated from 0 to 200 °C at a heating rate of 10 °C/min; nitrogen gas was used for purging. Residual weight as a function of temperature was recorded. The content of residual solvents was calculated from the weight loss between 0 to 120 °C as compared to the weight of the original sample mass.

**2.3.5. X-ray Diffraction (XRD).** X-ray diffraction patterns of gefitinib free base, PLGA 5004A, blank PLGA microspheres, and different gefitinib-loaded PLGA microspheres were recorded using a Bruker-AXS D8 ADVANCE diffractometer coupled with a VANTEC detector and a Ni filter. The measurements were made using Co-K $\alpha_{12}$  radiation ( $\lambda = 1.79026$  Å) at ambient conditions. Scans were performed between 10–75° 2 theta (2 $\theta$ ), using a step size of 0.09° 2 $\theta$  and a scan speed of 2 s. Separate blank patterns were recorded to allow subtraction of air and capillary wall-scattering. Three individual small angle XRD measurements were performed.

**2.3.6. Differential Scanning Calorimetry (DSC).** The physical state of the drug in the microspheres was analyzed using differential scanning calorimetry (DSC, Q2000, TA Instruments, USA). Samples of 3–10 mg (accurately weighed) of freeze-dried microspheres were loaded into aluminum pans and were subsequently closed. Samples were exposed to a three cycle heating/cooling protocol. In detail, the samples were heated from 0 to 60 °C at a heating rate of 10 °C/min. Next, the samples were cooled down to 0 °C at a rate of 100 °C/min. After 5 min at temperature 0 °C, the samples were heated again to 220 °C at a heating rate of 10 °C/min and a temperature modulation  $\pm 1$  °C/30 s. The melting temperature ( $T_m$ ) was determined from the total heat flow of the second heating ramp, and the glass transition temperature ( $T_g$ ) was determined from the reverse heat flow from the first and second heating ramps. Analysis of the results was carried out by TA Instruments Universal Analysis software. Physical mixtures of the PLGA and gefitinib base were analyzed by DSC to determine the limit of detection of this technique for gefitinib crystallinity in PLGA matrixes.

**2.4. In Vitro Release of Gefitinib from PLGA Microspheres.** *In vitro* drug release experiments were performed with microspheres embedded in dextran–methacrylate (Dex–MA) hydrogels to prevent their aggregation during the incubation conditions, while not limiting the release of gefitinib from the polymeric microparticles. Methacrylated dextran T40 (Mw 32.5k Da) with a degree of substitution of 10 was synthesized using a previously described procedure and used to form chemically cross-linked hydrogels by free radical polymerization.<sup>29,30</sup> In brief, gefitinib-loaded PLGA microspheres (3 mg) were dispersed in a solution of methacrylated dextran (150 mg dissolved in 1140  $\mu$ L of PBS (pH 7.4, 0.049 M NaH<sub>2</sub>PO<sub>4</sub>,

0.099 M Na<sub>2</sub>HPO<sub>4</sub>, 0.006 M NaCl) containing 0.05% w/w sodium azide). Polymerization was initiated by addition of 135  $\mu$ L of potassium persulfate solution (KPS; 50 mg/mL in PBS; 17  $\mu$ mol of KPS/g of gel) and 75  $\mu$ L tetramethylethylenediamine solution (TEMED 75  $\mu$ L; 20% (v/v) in PBS; 67  $\mu$ mol/g of gel).

Dispersion of gefitinib-loaded microspheres in 5 mm thick hydrogel slices (surface area = 0.6 cm<sup>2</sup>) was visualized by fluorescence microscopy (Leica DM IRB, Germany). Excitation of gefitinib at 345 nm and emission at 385–465 nm were recorded.<sup>31</sup>

*In vitro* release experiments were carried out in PBS containing 1% Tween 80 as incubation buffer to ensure sink conditions for the released gefitinib. The incubation buffer also contained 0.01% sodium azide to prevent bacterial growth. Dextran–MA hydrogels loaded with gefitinib microspheres (7.5 mg of microspheres corresponding to approximately 5 mg of gefitinib in 1 mL of dextran–MA hydrogel) were casted in Slide-A-Lyzer MINI Dialysis Devices (2K MWCO, external diameter = 0.86 cm, length = 1.73 cm Thermo scientific). An equivalent amount of gefitinib free base crystals were loaded in dextran–MA hydrogels to verify that release rates were dependent on drug release from microspheres and not on dissolution or diffusion of drug from the hydrogel. After solidification of the Dex–Ma solution, the dialysis devices were transferred into centrifugation tubes containing 15 mL of PBS buffer (1% Tween 80) and incubated at 37 °C under constant shaking. At different time points, 1 mL of the buffer was sampled and replaced by fresh buffer. The concentration of gefitinib in the release samples was determined by HPLC as described in section 2.3.2. Cumulative gefitinib release was fitted by linear and nonlinear regression analysis (Graphpad Prism version 5) according to eq 1 (zero-order release model, small microspheres < 50  $\mu$ m) or according to eq 2 (sigmoidal release model according to Duvvuri et al.;<sup>33</sup> microspheres > 50  $\mu$ m and unfractionated microspheres).

$$Q = A + kt \quad (1)$$

In which  $Q$  stands for cumulative drug release,  $t$  stands for the time since start of the release experiment,  $A$  is the intercept with Y-axis (burst release), and  $k$  is the rate constant of release.

$$Q = A(1 - e^{-k_1 t}) + \frac{B}{1 + e^{-k_2(t-T_{50})}} \quad (2)$$

In which  $Q$  stands for cumulative drug release,  $t$  stands for the time since start of the release experiment,  $A$  is the percentage of total drug released during phase I,  $k_1$  is the rate constant of drug release during phase I,  $B$  is the percentage of total drug released during phase II,  $k_2$  is the rate constant of drug release during phase II, and  $T_{50}$  is the time taken to release 50% of entrapped drug.

The best fitted line for the unfractionated microspheres from the individual weight fractions was also calculated.

**2.5. In Vitro Degradation of Microspheres.** Aliquots of gefitinib-loaded or placebo microspheres (5 mg) were transferred into 1.5 mL Eppendorf tubes and dispersed in 1 mL of incubation buffer (see section 2.3.2). Samples were incubated at 37 °C while gently shaking. At different time points, tubes were taken out of the incubator and centrifuged at 20,000g for 20 min to collect the microspheres. The pelleted microspheres were washed twice with 1 mL of reverse osmosis water and subsequently lyophilized and weighed. Morphology of the incubated microspheres was studied by SEM as described in



**Table 1.** Properties of Gefitinib-Loaded PLGA Microspheres<sup>a</sup>

formulations	particle size <sup>b</sup> ( $\mu\text{m}$ )	span value <sup>c</sup>	EE <sup>d</sup> (%)	LC <sup>e</sup> (%)	yield <sup>f</sup> (%)
unfractionated	59 $\pm$ 10	1.5 $\pm$ 0.3	70.1 $\pm$ 3.6	6.3 $\pm$ 0.4	81.0 $\pm$ 1.7
sieved					
<20 $\mu\text{m}$	5 $\pm$ 1	0.4 $\pm$ 0.1	33.4 $\pm$ 4.0	2.4 $\pm$ 0.3	14.0 $\pm$ 1.7
20–50 $\mu\text{m}$	32 $\pm$ 4	0.7 $\pm$ 0.2	64.3 $\pm$ 3.6	5.8 $\pm$ 0.3	18.0 $\pm$ 1.7
50–100 $\mu\text{m}$	70 $\pm$ 3	0.6 $\pm$ 0.3	82.1 $\pm$ 4.7	7.3 $\pm$ 0.4	31.0 $\pm$ 3.0
>100 $\mu\text{m}$	130 $\pm$ 7	0.9 $\pm$ 0.2	84.2 $\pm$ 5.6	7.6 $\pm$ 0.9	35.0 $\pm$ 2.7

<sup>a</sup>Mean  $\pm$  SD values were calculated from the data of three independently prepared batches and represent reproducibility between batches. <sup>b</sup>Particle size expressed as volume weighted mean diameter. <sup>c</sup>Span value =  $(d_{90} - d_{10})/d_{50}$ , which reflects the polydispersity within individual batches and size fractions. <sup>d</sup>EE: Encapsulation efficiency of gefitinib <sup>e</sup>LC: loading content of gefitinib in the collected polymeric microspheres <sup>f</sup>Yields were calculated as % of the original materials (unfractionated microspheres) or relative to amount of material before sieving (fractionated microspheres)

section 2.3.3, while the polymer molecular weights were determined using gel permeation chromatography on a Waters Alliance system equipped with a refractive index detector. Two-PL-gel 5  $\mu\text{m}$  Mixed-D columns fitted with a guard column (Polymer Laboratories, Mw range = 0.2–400 kDa) were used, and calibration was done using polystyrene standards with narrow molecular weight distributions. THF was used as the mobile phase (1 mL/min).

### 3. RESULTS AND DISCUSSION

#### 3.1. Encapsulation of Gefitinib in PLGA Microspheres.

Since gefitinib has a low solubility in DCM of approximately 15 mg/mL, DMSO was used as cosolvent for the O/W emulsification, affording a theoretical drug loading of 9% w/w. Microspheres were obtained with an average size of 59  $\mu\text{m}$  and a gefitinib loading content of 6.3% w/w (70% EE), as listed in Table 1. The overall yield after lyophilization was 81% of the starting materials. The obtained batches of gefitinib microspheres were sieved into 4 size-fractions with good recovery for both drug and polymeric materials (98%) and no drug detectable in the washing fluids. The two largest size-fractions (50–100  $\mu\text{m}$  and >100  $\mu\text{m}$ ) represented 66% of the collected material.

Interestingly, the drug loading content (LC) differed significantly among the different size-fractions, with more than a 3-fold difference between the largest and smallest size-fractions. Since the recovery of the drug was 98% after wet sieving, the lower LC of the smaller size fractions reflects differences in drug loading between smaller and larger sized microspheres that had been established already before sieving of the unfractionated material, i.e., during the emulsification and solvent extraction phases. Siepmann et al. also found similar results for 5-fluorouracil (5-FU) microparticles prepared by a solid-in-oil-in-water emulsification process.<sup>15</sup> Although their results could be explained by entrapment of more and relatively larger drug particles in the larger oil droplets versus small droplets, this does not apply to our data on gefitinib PLGA microparticles since the drug was dissolved in the DCM/DMSO phase before emulsification. A possible explanation for our results is that drug loss during emulsification is mainly due to partitioning of gefitinib from the dispersed oil droplets into the external water phase. Such processes will mainly occur at the surface of the polymer droplets when the particles have not solidified yet. Once the particles have solidified, the drug will be entrapped in the polymer matrix. The relative higher surface:volume ratio of smaller droplets will result in relative higher drug loss and hence a lower EE for smaller microparticles.

#### 3.2. Morphological Characterization of Gefitinib Microspheres.

Figure 2 shows the SEM micrographs of the unfractionated and sieved gefitinib-loaded PLGA microspheres. All gefitinib-loaded PLGA microspheres had a smooth and nonporous surface, without the presence of surface localized drug crystals. It is also evident from the images that the

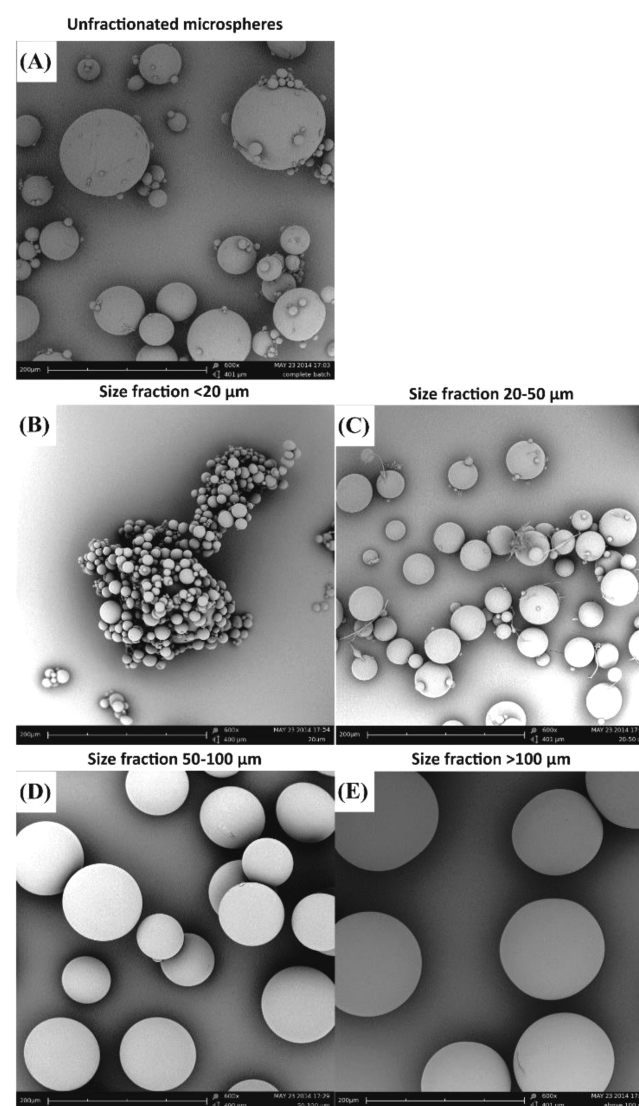


**Figure 2.** SEM micrographs of (A) unfractionated gefitinib PLGA microspheres and (B–E) size-fractionated gefitinib-loaded PLGA microspheres: (B) <20  $\mu\text{m}$ ; (C) 20–50  $\mu\text{m}$ ; (D) 50–100  $\mu\text{m}$ ; and (E) >100  $\mu\text{m}$ ; 600 $\times$  magnification.

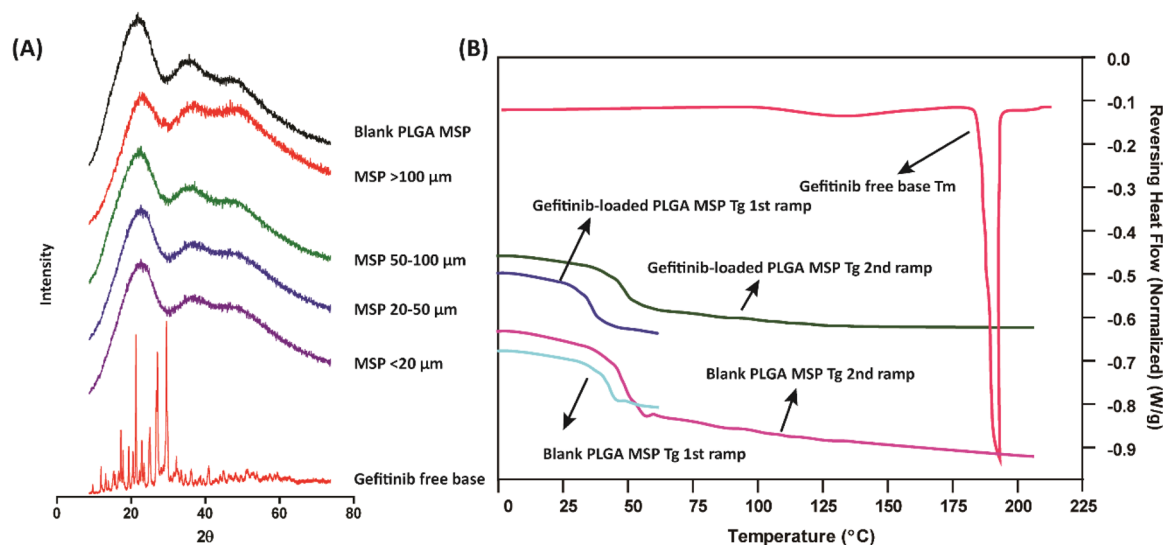


**Figure 3.** X-ray diffraction patterns of gefitinib free base, blank PLGA microspheres, and gefitinib-loaded PLGA microspheres with different size fractions (A). DSC profile of gefitinib-free base, blank microspheres, and gefitinib-loaded PLGA microspheres (B).

unfractionated sample contained both small and larger microspheres, whereas the fractionated samples A–D primarily contained microspheres within the specified ranges, consistent with the size distribution data in Table 1. Minor amounts of small particles were however detected in the sieved fractions. Most likely, this is due to hydrophobic nature of PLGA, which favors adherence of small microparticles to larger ones during the wet-sieving process. Size distributions of the gefitinib-loaded PLGA microspheres are shown in Figure S1.

**3.3. XRD and Thermal Analysis.** The physical state of gefitinib in PLGA microspheres was studied by XRD crystallography, as shown in Figure 3A. Gefitinib-free base is highly crystalline and exhibited intense peaks at 18.6°, 19.2°, 24.2°, 26.2° and 26.4° as also reported by Lee et al.<sup>32</sup> PLGA microspheres prepared without drug (blank microspheres) showed no peak indicative of crystalline material, which is expected for fully amorphous PLGA. Gefitinib-loaded microspheres did not show peaks indicative for the presence of crystalline drug, although one should note that the detection limit of XRD (5% w/w gefitinib in PLGA) is close to the drug loading content in the microspheres.

Modulated DSC was applied to further investigate the physical state of the dispersed gefitinib in the PLGA microspheres. The thermogram of gefitinib (Figure 3B) showed an endothermic peak at 195 °C ( $\Delta H = 130.1$  J/g) corresponding to its melting temperature.<sup>32</sup> The melting peak of gefitinib was not detected in the thermograms of gefitinib-loaded PLGA microspheres, which confirms the absence of crystalline drug within the polymeric microparticles, similar to the XRD data. DSC analysis of a physical mixture of gefitinib and PLGA demonstrated that DSC is able to detect the melting behavior of gefitinib in the same weight proportion as the drug loading content in PLGA microspheres (7% w/w) (Supplemental Figure S2); the melting enthalpy of the drug corresponded to the expected weight fraction of the drug. These data indicate that gefitinib is either molecularly or amorphously dispersed in the matrix of the microspheres. The  $T_g$  of PLGA in the second heating cycle was not significantly different between blank and gefitinib-loaded microparticles (44 °C, Table 2 and Figure 3), although lower  $T_g$  values were recorded in the first heating ramp until 60 °C for both blank

**Table 2.** Thermal Analysis of Unfractionated and Fractionated Gefitinib-Loaded PLGA Microspheres Using DSC<sup>a</sup>

samples	$T_g$ 1st run (°C)	$T_g$ 2nd run (°C)
unfractionated	34.2 ± 0.1	44.1 ± 0.7
MSP <20 μm	40.3 ± 0.2	43.2 ± 0.2
MSP 20–50 μm	38.1 ± 0.1	44.2 ± 0.5
MSP 50–100 μm	34.8 ± 0.3	42.3 ± 0.3
MSP >100 μm	34.3 ± 0.2	43.1 ± 0.5

<sup>a</sup>Data are expressed as mean ± SD ( $n = 3$ ).

and drug-loaded microparticles. Such differences between first and second heating cycle are indicative of the evaporation of residual solvents from the studied materials, which was confirmed by measuring the weight loss by thermogravimetric analysis in the same heating range (60–120 °C) where thermal decomposition of drug and PLGA is not yet expected. Since the weight loss (less than 1%) was mainly observed above 60 °C but below 120 °C, i.e., above the evaporation temperature of DCM but below the evaporation temperature of DMSO, we attributed the weight loss to evaporation of water. Apparently, small amounts of water were present in the PLGA matrix even after two subsequent lyophilization steps. More importantly, since all differences in  $T_g$  between naive PLGA 5004A and drug-loaded microspheres disappeared in the second heating ramp, we concluded that gefitinib was amorphously but not molecularly dissolved in the polymeric matrix since the latter case would infer a decrease in  $T_g$  of the polymer due to plasticizing effects.

**3.4. In Vitro Release of Gefitinib from Hydrogel Embedded Microspheres.** Microspheres were embedded in dextran–MA hydrogels to avoid their aggregation during release experiments. Supplemental Figure S3 shows that gefitinib release from such hydrogels was relatively fast and reached equilibrium after 1 h, thus demonstrating that dextran–MA hydrogels will not affect the release profiles obtained from the polymeric microparticles.

Size-fractionated microspheres showed remarkable differences in drug release between small microspheres and larger microspheres (Figure 4). Microspheres of size-fractions A and

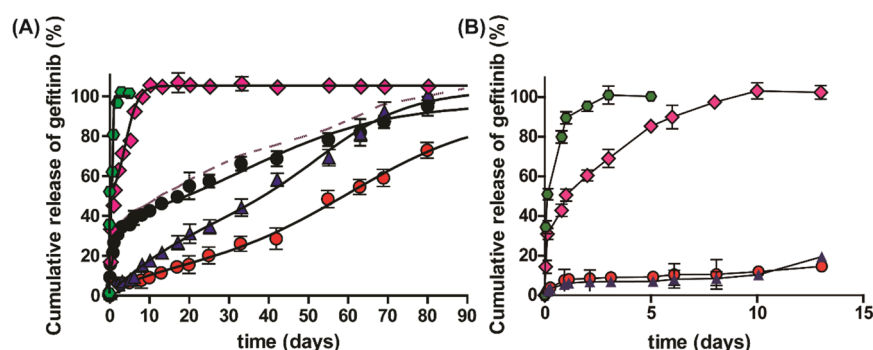


**Figure 4.** *In vitro* release of gefitinib-loaded PLGA microspheres. (A) Closed black circles represent the unfractionated microspheres, green hexagons and pink diamonds represent smaller size fractions A (<20  $\mu\text{m}$ ) and B (20–50  $\mu\text{m}$ ); blue triangles and red circles represent larger microspheres 50–100 and >100  $\mu\text{m}$  of gefitinib-loaded PLGA microspheres. The lines drawn represent linear or nonlinear regression fit according to eqs 1 and 2. The purple dotted line represents the theoretical release profile of the combined batches of <20, 20–50, 50–100, and >100  $\mu\text{m}$  gefitinib-loaded PLGA microspheres (weight fractions as reported in Table 1). (B) Zoom out of graph A for the early time release. Data are expressed as mean  $\pm$  SD ( $n = 3$ ).

**Table 3.** Nonlinear Sigmoidal Regression Analysis of Release Curves<sup>a</sup>

fitted parameter	unfractionated gefitinib microspheres	fraction A: <20 $\mu\text{m}$	fraction B: 20–50 $\mu\text{m}$	fraction C: 50–100 $\mu\text{m}$	fraction D: >100 $\mu\text{m}$
A (% release)	29.60	53.32	43.26	19.38	12.75
$k_1$ ( $\text{day}^{-1}$ )	0.70	24.86	7.02	0.04	0.07
B (% release)	66.89	45.59	59.65	80.42	87.25
$k_2$ ( $\text{day}^{-1}$ )	0.06	9.21	4.13	0.09	0.06
$T_{50}$ (day)	33.87	0.96	4.13	53.76	60.62
$R^2$	0.9783	0.9929	0.9853	0.9822	0.9814

<sup>a</sup>Best-fit value of cumulative release from gefitinib-loaded PLGA microspheres. Corresponding curves are shown in Figure 6.

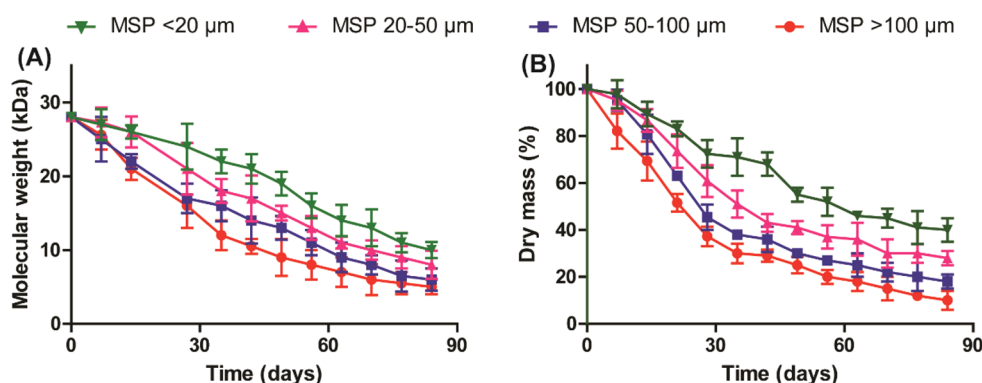


**Figure 5.** Degradation of gefitinib-loaded PLGA microspheres with different sizes. (A) Changes in the  $M_n$  (kDa) upon *in vitro* incubation. (B) Dry mass loss of the same samples.

B, i.e., <20 and 20–50  $\mu\text{m}$ , respectively, showed complete release within 1 week, while larger microspheres showed slow release in the first week (<20% cumulative release for fraction C (50–100  $\mu\text{m}$ ); <10% cumulative release for fraction D (>100  $\mu\text{m}$ )). In contrast, these larger microspheres showed a sigmoidal release profile that leveled off after the initial burst and accelerated from day 30 until the end of the incubation at 3 months. Fitted parameters of the release data are shown in Table 3 and represent nonlinear sigmoidal regression analysis according to eq 2. In the empirical model for sigmoidal drug release, as mentioned in section 2.4, constants A and B represent the relative proportion of drug release during phase I and phase II of the curves,  $T_{50}$  represents the time point at which 50% of the drug has been released, and time constants  $k_1$  and  $k_2$  reflect the drug release rate during phase I and phase II. Microspheres of size-fraction D showed an average release rate of 6.1%/day ( $B \times k_2$ ) while size-fraction C displayed an average

release rate of 7.2%/day in the later phases of the release study. The mathematically reconstituted release curve for non-fractionated gefitinib microspheres, as calculated from the relative weight percentages of the fractions and the individual release curves, matched very well with the observed release profile of the unfractionated gefitinib microspheres. Since weight fractions C and D represented 66% of the total material, these larger microspheres largely determined the sustained phase of the reconstituted release curve, while drug release in the first 2 weeks could be mainly attributed to the smaller size fractions. Moreover, our results also demonstrate that burst release mainly originates from the smaller microspheres, rather than release of surface bound drug from all microparticles.

Although one can expect slower drug release from larger microparticles due to the increase in diffusion path lengths, the striking differences in release profiles overrule a simple relationship solely based on diffusion behavior of gefitinib in



the polymeric matrix. Moreover, one would expect similarly shaped profiles when they had been guided by the same release principle. It is therefore more likely that a complex interplay of drug dissolution, drug and water diffusion, and polymer degradation affects drug release during the different phases of the release profiles.

**3.5. Polymer Degradation Behavior.** The gradual degradation of the PLGA microparticles upon *in vitro* incubation is shown in Figure 5, either showing the number-average molecular weight ( $M_n$ ; panel A) as determined by gel permeation chromatography or the residual weight of the microspheres (panel B). PLGA degradation is accelerated upon lowering of the microclimate pH within the core of the microparticles.<sup>3,33,34</sup> The observed faster degradation of larger microparticles thus can be explained by the autocatalytic degradation of PLGA, in which the retention of acidic degradation within these larger microspheres results in a more pronounced and faster cleavage of the ester bonds in the polymer chains. Despite the observed slower degradation of the smaller size-fractions, this did not affect the release profiles since these particles already have lost most of the encapsulated drug before pronounced erosion starts.

Erosion of the microspheres was also reflected by the SEM micrographs that were collected during the first 4 weeks of the degradation study as shown in Figure 6. Erosion of the

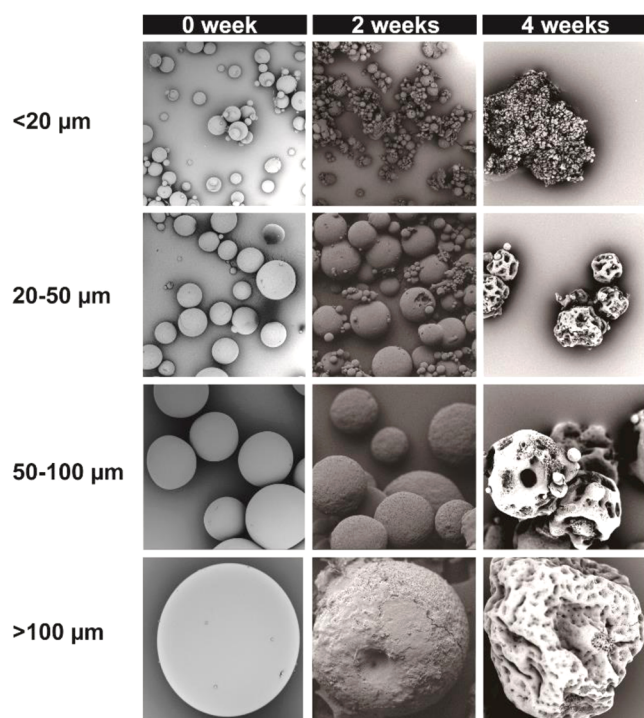


**Figure 6.** SEM micrographs of gefitinib-loaded PLGA microspheres upon *in vitro* incubation in buffer of pH 7.4 and at 37 °C. The magnification is  $\times 1200$  for all images.

microspheres was observed at 2 weeks incubation and increased with increasing exposure time due to polymer degradation. Upon 4 weeks of incubation, pores had formed on the coarse surface of the particles and bulk erosion had altered the shape and surface of the particles.

Previous studies have reported a clear relationship between microparticle size and drug release and degradation kinetics.<sup>13</sup> Our results are in good agreement with the results obtained by

Berkland et al., who found that monodisperse piroxicam-loaded PLGA microspheres with smaller diameter ( $\sim 10 \mu\text{m}$ ) exhibited diffusion-controlled drug release, while larger particles (50 and 100  $\mu\text{m}$ ) exhibited a sigmoidal release profile.<sup>13</sup> Remarkably, the release window of our gefitinib-loaded microspheres in the same size ranges (50–100 and  $>100 \mu\text{m}$ ) was around 80 days, while the piroxicam microspheres exhibited complete release within 2 weeks. Plausible explanations for these differences are the much higher water solubility of piroxicam versus gefitinib (around 1000-fold difference; 23 mg/mL and 27  $\mu\text{g/mL}$ , respectively), and the lower PLGA molecular weight (13,000 vs 28,000 g/mol).

Apart from their size, the presently prepared microspheres differed in their drug-loading content, which may also have contributed to differences in drug release profiles between the size fractions. In a study with 5-fluorouracil-loaded PLGA microspheres, higher drug loadings of larger microparticles correlated to a faster drug release rate that was attributed to an increase in internal porosity upon drug depletion.<sup>14</sup> In our study, however, larger microspheres showed slower drug release, i.e., an inverse relationship between drug loading content and release rate. Moreover, we observed a much longer release window for gefitinib microspheres than was observed for 5-FU microspheres. A plausible explanation is the more hydrophobic character of gefitinib that, for instance, can retard the effect of water influx into the particles; as a consequence, drug dissolution will be more retarded at higher drug loading content.

Another factor that can explain sigmoidal drug release profiles is the drug distribution within the microspheres. The aforementioned piroxicam PLGA microspheres displayed a sigmoidal release profile and had a nonuniform drug distribution in larger microspheres (50  $\mu\text{m}$ ), while small microspheres (10  $\mu\text{m}$ ) particles showed uniform drug distribution and diffusion-like release profiles.<sup>17</sup> A nonuniform drug distribution and sigmoidal release profiles were also reported for paclitaxel microspheres.<sup>35</sup> In our present research, the sigmoidal release profile of the bigger microspheres (50–100  $\mu\text{m}$  and  $>100 \mu\text{m}$ ) and higher drug loading content may also reflect nonuniform drug distribution in the microspheres.

Sansdrap et al. also found similar results as we observed for nifedipine microspheres. The nifedipine microspheres with sizes of 18 and 80  $\mu\text{m}$  had completely different release behavior: the profiles obtained were almost linear after 1-day burst effect for 18  $\mu\text{m}$  and biphasic for 80  $\mu\text{m}$  microspheres.<sup>36</sup> According to their swelling data, water uptake by the 18  $\mu\text{m}$  microspheres was much higher than for the 80  $\mu\text{m}$  microspheres (170% swelling increase versus 125% in 3 days). The water content in turn influenced the ability of active component to diffuse through the matrix by increasing polymer permeability. In our study, the swelling rate can be also different among the smaller and larger microspheres, which consequentially affects the permeability of the polymer matrix and the drug release rate.

## 4. CONCLUSIONS

The results of the present study demonstrate that polydisperse drug-loaded microspheres differ in multiple aspects that influence drug release. Separating polydisperse microspheres into sieve fractions allowed us to demonstrate remarkable differences in drug release mechanism between smaller and larger microparticles from the same drug–polymer o/w emulsion and also eliminated most of the initial burst release.

Thus, sieve-fractionating of polydisperse microspheres is a relative simple and effective procedure to obtain drug-releasing microparticles with better defined release properties and allows for further tailoring when sieve fractions are recombined to reconstitute the desired release profile.

## ■ ASSOCIATED CONTENT

### ■ Supporting Information

The Supporting Information is available free of charge on the ACS Publications website at DOI: [10.1021/acs.molpharmaceut.6b00896](https://doi.org/10.1021/acs.molpharmaceut.6b00896).

Particle size distributions of gefitinib-loaded PLGA microspheres, DSC thermogram of physical mixture of gefitinib crystals (7% w/w) and PLGA, release curve of gefitinib from dextran–MA gel (PDF)

## ■ AUTHOR INFORMATION

### Corresponding Author

\*Phone: + 31 620275995. Fax: + 31 30 251789. E-mail: [r.j.kok@uu.nl](mailto:r.j.kok@uu.nl).

### ORCID

Robbert J. Kok: [0000-0003-4933-3968](https://orcid.org/0000-0003-4933-3968)

### Notes

The authors declare no competing financial interest.

## ■ ACKNOWLEDGMENTS

The authors would like to acknowledge the financial support from European Union's Seventh Framework Program under grant agreement NMP3-SL-2012-280915 (Pulmostent). Marjan Versluijs-Helder is kindly acknowledged for assistance with the XRD experiments.

## ■ REFERENCES

- (1) Ma, G. Microencapsulation of protein drugs for drug delivery: strategy, preparation, and applications. *J. Controlled Release* **2014**, *193*, 324–340.
- (2) Ansary, R. H.; Awang, M. B.; Rahman, M. M. Biodegradable poly (D, L-lactic-co-glycolic acid)-based micro/nanoparticles for sustained release of protein drugs-A review. *Trop. J. Pharm. Res.* **2014**, *13*, 1179–1190.
- (3) Liu, Y.; Schwendeman, S. P. Mapping microclimate pH distribution inside protein-encapsulated PLGA microspheres using confocal laser scanning microscopy. *Mol. Pharmaceutics* **2012**, *9*, 1342–1350.
- (4) Prajapati, V. D.; Jani, G. K.; Kapadia, J. R. Current knowledge on biodegradable microspheres in drug delivery. *Expert Opin. Drug Delivery* **2015**, *12*, 1283–1299.
- (5) Ramazani, F.; Chen, W.; van Nostrum, C. F.; Storm, G.; Kiessling, F.; Lammers, T.; Hennink, W. E.; Kok, R. J. Strategies for encapsulation of small hydrophilic and amphiphilic drugs in PLGA microspheres: state-of-the-art and challenges. *Int. J. Pharm.* **2016**, *499*, 358–367.
- (6) Zhang, Y.; Wischke, C.; Mittal, S.; Mitra, A.; Schwendeman, S. P. Design of controlled release PLGA microspheres for hydrophobic fenretinide. *Mol. Pharmaceutics* **2016**, *13*, 2622–2630.
- (7) Wischke, C.; Schwendeman, S. P. Principles of encapsulating hydrophobic drugs in PLA/PLGA microparticles. *Int. J. Pharm.* **2008**, *364*, 298–327.
- (8) Crotts, G.; Park, T. G. Preparation of porous and nonporous biodegradable polymeric hollow microspheres. *J. Controlled Release* **1995**, *35*, 91–105.
- (9) Freitas, S.; Merkle, H. P.; Gander, B. Microencapsulation by solvent extraction/evaporation: reviewing the state of the art of microsphere preparation process technology. *J. Controlled Release* **2005**, *102*, 313–332.
- (10) Nakashima, T.; Shimizu, M.; Kukizaki, M. Membrane emulsification by microporous glass. *Key Eng. Mater.* **1992**, *61*, 513–516.
- (11) Kazazi-Hyseni, F.; Landin, M.; Lathuile, A.; Veldhuis, G. J.; Rahimian, S.; Hennink, W. E.; Kok, R. J.; van Nostrum, C. F. Computer modeling assisted design of monodisperse PLGA microspheres with controlled porosity affords zero order release of an encapsulated macromolecule for 3 months. *Pharm. Res.* **2014**, *31*, 2844–2856.
- (12) Nakashima, T.; Shimizu, M.; Kukizaki, M. Particle control of emulsion by membrane emulsification and its applications. *Adv. Drug Delivery Rev.* **2000**, *45*, 47–56.
- (13) Berkland, C.; King, M.; Cox, A.; Kim, K. K.; Pack, D. W. Precise control of PLG microsphere size provides enhanced control of drug release rate. *J. Controlled Release* **2002**, *82*, 137–147.
- (14) Siepmann, J.; Faisant, N.; Akiki, J.; Richard, J.; Benoit, J. Effect of the size of biodegradable microparticles on drug release: experiment and theory. *J. Controlled Release* **2004**, *96*, 123–134.
- (15) Berkland, C.; Kim, K. K.; Pack, D. W. Fabrication of PLG microspheres with precisely controlled and monodisperse size distributions. *J. Controlled Release* **2001**, *73*, 59–74.
- (16) Samadi, N.; Abbadessa, A.; Di Stefano, A.; van Nostrum, C. F.; Vermonden, T.; Rahimian, S.; Teunissen, E.; van Steenberg, M. J.; Amidi, M.; Hennink, W. E. The effect of lauryl capping group on protein release and degradation of poly (D, L-lactic-co-glycolic acid) particles. *J. Controlled Release* **2013**, *172*, 436–443.
- (17) Raman, C.; Berkland, C.; Kim, K. K.; Pack, D. W. Modeling small-molecule release from PLG microspheres: effects of polymer degradation and nonuniform drug distribution. *J. Controlled Release* **2005**, *103*, 149–158.
- (18) Casalini, T.; Rossi, F.; Lazzari, S.; Perale, G.; Masi, M. Mathematical modeling of PLGA microparticles: from polymer degradation to drug release. *Mol. Pharmaceutics* **2014**, *11*, 4036–4048.
- (19) Sevim, K.; Pan, J. A mechanistic model for acidic drug release using microspheres made of PLGA 50:50. *Mol. Pharmaceutics* **2016**, *13*, 2729–2735.
- (20) Costa, P.; Lobo, J. M. S. Modeling and comparison of dissolution profiles. *Eur. J. Pharm. Sci.* **2001**, *13*, 123–133.
- (21) Siepmann, J.; Siepmann, F. Modeling of diffusion controlled drug delivery. *J. Controlled Release* **2012**, *161*, 351–362.
- (22) Siepmann, J.; Göpferich, A. Mathematical modeling of bioerodible, polymeric drug delivery systems. *Adv. Drug Delivery Rev.* **2001**, *48*, 229–247.
- (23) Duvvuri, S.; Janoria, K. G.; Mitra, A. K. Effect of polymer blending on the release of ganciclovir from PLGA microspheres. *Pharm. Res.* **2006**, *23*, 215–223.
- (24) Reck, M.; Heigener, D. F.; Mok, T.; Soria, J.-C.; Rabe, K. F. Management of non-small-cell lung cancer: recent developments. *Lancet* **2013**, *382*, 709–719.
- (25) Ramazani, F.; Chen, W.; van Nostrum, C. F.; Storm, G.; Kiessling, F.; Lammers, T.; Hennink, W. E.; Kok, R. J. Formulation and characterization of microspheres loaded with imatinib for sustained delivery. *Int. J. Pharm.* **2015**, *482*, 123–130.
- (26) O'Donnell, P. B.; McGinity, J. W. Preparation of microspheres by the solvent evaporation technique. *Adv. Drug Delivery Rev.* **1997**, *28*, 25–42.
- (27) El-Mahdy, M.; Ibrahim, E.-S.; Safwat, S.; El-Sayed, A.; Ohshima, H.; Makino, K.; Muramatsu, N.; Kondo, T. Effects of preparation conditions on the monodispersity of albumin microspheres. *J. Microencapsulation* **1998**, *15*, 661–673.
- (28) Guo, W.; Quan, P.; Fang, L.; Cun, D.; Yang, M. Sustained release donepezil loaded PLGA microspheres for injection: preparation, in vitro and in vivo study. *Asian J. Pharm. Sci.* **2015**, *10*, 405–414.
- (29) van Dijk-Wolthuis, W. N.; Franssen, O.; Talsma, H.; van Steenberg, M. J.; Kettenes-Van Den Bosch, J.; Hennink, W. E. Synthesis, characterization, and polymerization of glycidyl methacrylate derivatized dextran. *Macromolecules* **1995**, *28*, 6317–6322.



- (30) van Dijk-Wolthuis, W.; Kettenes-Van Den Bosch, J.; Van Der Kerk-Van Hoof, A.; Hennink, W. Reaction of dextran with glycidyl methacrylate: an unexpected transesterification. *Macromolecules* **1997**, *30*, 3411–3413.
- (31) Rahimian, S.; Fransen, M. F.; Kleinovink, J. W.; Amidi, M.; Ossendorp, F.; Hennink, W. E. Polymeric microparticles for sustained and local delivery of antiCD40 and antiCTLA-4 in immunotherapy of cancer. *Biomaterials* **2015**, *61*, 33–40.
- (32) Phillip Lee, Y. H.; Sathigari, S.; Jean Lin, Y. J.; Ravis, W. R.; Chadha, G.; Parsons, D. L.; Rangari, V. K.; Wright, N.; Babu, R. J. Gefitinib-cyclodextrin inclusion complexes: physico-chemical characterization and dissolution studies. *Drug Dev. Ind. Pharm.* **2009**, *35*, 1113–1120.
- (33) Vert, M.; Schwach, G.; Engel, R.; Coudane, J. Something new in the field of PLA/GA bioresorbable polymers? *J. Controlled Release* **1998**, *53*, 85–92.
- (34) Anderson, J. M.; Shive, M. S. Biodegradation and biocompatibility of PLA and PLGA microspheres. *Adv. Drug Delivery Rev.* **1997**, *13*, 5–24.
- (35) Elkharraz, K.; Faisant, N.; Guse, C.; Siepmann, F.; Arica-Yegin, B.; Oger, J. M.; Gust, R.; Goepferich, A.; Benoit, J. P.; Siepmann, J. Paclitaxel-loaded microparticles and implants for the treatment of brain cancer: preparation and physicochemical characterization. *Int. J. Pharm.* **2006**, *314*, 127–136.
- (36) Sansdrap, P.; Moës, A. J. In vitro evaluation of the hydrolytic degradation of dispersed and aggregated poly (DL-lactide-co-glycolide) microspheres. *J. Controlled Release* **1997**, *43*, 47–58.